The Spingosine-1-Phosphate Analogue FTY720 Impairs Mucosal Immunity and Clearance of the Enteric Pathogen *Citrobacter rodentium*

Carola T. Murphy[1], Lindsay J. Hall[1,%], Grainne Hurley[1], Aoife Quinlan[1], John MacSharry[1], Fergus Shanahan[1], Kenneth Nally[1#], Silvia Melgar[1#]*

[1]Alimentary Pharmabiotic Centre, University College Cork, National University of Ireland, Cork, Ireland.

Running Title: FTY720 impairs immune responses to infection.

***Corresponding Author:**

Silvia Melgar, PhD
Tel. +353-21-4901384
Fax: +353-21-4901436
Email: s.melgar@ucc.ie

Abstract

The sphingosine-1-phosphate (S1P) analogue, FTY720, is therapeutically efficacious in multiple sclerosis and in the prevention of transplant rejection. It prevents migration of lymphocytes to sites of pathology by trapping them within the peripheral lymph nodes, the mesenteric lymph nodes (MLNs) and Peyer's patches. However, evidence suggests that its clinical use may increase the risk of mucosal infections. We investigated the impact of FTY720 treatment on susceptibility to gastrointestinal infection with the mouse enteric pathogen, *Citrobacter rodentium (C. rodentium)*. This attaching and effacing bacterium induces a transient bacterial colitis in immunocompetent mice, which resembles human infection with pathogenic *Escherichia coli*. FTY720 treatment induced peripheral blood lymphopenia, trapped lymphocytes in the MLNs and prevented clearance of bacteria when mice were infected with *luciferase*-tagged *C. rodentium*. FTY720-treated *C. rodentium*-infected mice had enhanced colonic inflammation, with significantly higher colon mass, colon histopathology and neutrophil infiltration, when compared with vehicle-infected animals. In addition, FTY720-treated infected mice had significantly lower numbers of colonic dendritic cells, macrophages and T cells. Gene expression analysis demonstrated that FTY720-treated infected mice had an impaired innate immune response and a blunted mucosal adaptive immune response including Th1 cytokines. . The data demonstrate that the S1P analogue, FTY720, adversely affects the immune response and clearance of *C. rodentium.*

INTRODUCTION

Therapeutic use of the Sphingosine 1–Phosphate (S1P) analogue FTY720 [Gilenya (fingolimod)] has proven efficacy in patients with multiple sclerosis (MS), and was recently approved by the US Food and Drug Administration as a first line treatment for relapsing forms of the disease (1, 27). FTY720 modulates S1P signalling, preventing lymphocyte egress from the thymus and spleen into the blood and from the lymph nodes (LNs) into the lymph, thus blocking lymphocyte trafficking to target tissues (5, 6, 16). It also affects dendritic cell (DC) migration (31), modulates DC pro-inflammatory signalling, and is a potent inhibitor of regulatory T cell (Treg) proliferation (56). Controversy surrounds the complex mechanism of action of FTY720 *in vivo* and it is unclear whether it acts as an agonist or functional antagonist or both during regulation of lymphocyte recirculation (21, 47, 52, 58). FTY720 ameliorated disease in numerous pre-clinical models of colitis including those induced by oxazolone (12), TNBS (11), DSS (14), adoptive transfer (14, 18) and in IL-10 deficient mice (36). In addition, it was therapeutically efficacious in graft versus host disease (24) and in clinical studies of transplantation and MS (2, 4, 23). However, treatment with FTY720 may increase the risk of mucosal infections and its effect on host immune responses upon exposure to such threats has yet to be completely elucidated. Two fatal herpes virus infections were reported in a clinical phase 3 study comparing FTY720 with IFN-β, (7, 19), and an increased incidence of respiratory tract infections, such as bronchitis, have been reported in MS patients with FTY720 treatment (8, 28). Nonetheless, studies to date assessing the effect of FTY720 on innate and adaptive immune responses have specifically focused on exposure to viral antigens and vaccines (30, 35). There are no studies examining the effect of FTY720 treatment following exposure to gastrointestinal infections.

In the current study, we assess the effect of continuous dosing of FTY720 on susceptibility of mice to *Citrobacter rodentium* (*C. rodentium*), a commonly used non-invasive enteropathogen, which is a model for human enteropathogenic *Escherichia coli* (EPEC) and enterohaemorrhagic *E. coli* (EHEC) infection. *C. rodentium* intimately attaches to the apical surface of the gut epithelium, inducing epithelial cell actin re-arrangements and localized destruction of brush border microvilli and leading to the formation of underlying pedestal-like attaching/effacing (A/E) lesions in the host cell (29). Oral infection of immunocompetent mice with *C. rodentium* leads to a transient colonisation and inflammation that peaks after one week and is cleared in the ensuing two to three weeks (37). Bacterial colonization is limited to the intestinal mucosa with low bacterial burden in systemic organs. The mice exhibit mild signs of clinical disease and microscopically the mucosa presents crypt hyperplasia, goblet cell loss and mucosal infiltration of immune cells including T cells, macrophages and neutrophils. For efficient bacterial clearance a robust Th1 host immune response is required, mediated by infiltrating $CD4^+$ T cells and macrophages. Thus, *C. rodentium* infection is an excellent model to investigate host-bacterial immune interactions in the intestine. In addition, the availability of a bioluminescent strain that allows pathogen burden and clearance dynamics to be followed *in vivo* using bioluminescence imaging makes this model a versatile tool (9, 17, 40). Our data clearly show that continuous treatment with FTY720 delays clearance of *C. rodentium* infection in mice, by blocking the migration of T cells and other immune cells to the inflamed colon. Host protective mucosal immunity is altered with impairment of innate and adaptive immune responses. This is the first report, to our knowledge, that FTY720 can compromise critical host defence against commonly encountered enteric pathogens.

MATERIALS AND METHODS

Mice

Specific pathogen-free female C57BL/6OlaHsD mice, 7–12 wk old, weighing 17–20 g, were obtained from Harlan, UK. All mice were housed in individually ventilated cages (IVCs, OptiMICE, Animal Care Systems, UK) in groups of 3-4 mice per cage, with sterile bedding, temperature 21°C, 12h light: 12h darkness, humidity 50% in a dedicated animal holding facility. They were fed a sterilized pellet diet and tap water *ad libitum*. Mice were allowed ≥2 wk to acclimatize before entering the study. All animal procedures were performed according to national ethical guidelines following approval by University College Cork Animal Experimentation Ethics Committee (AEEC).

Citrobacter rodentium- induced colitis

The bioluminescent *C. rodentium* strain ICC180, was a gift from Prof. Gordon Dougan (Wellcome Trust Sanger Institute, UK). This nalidixic acid (NA)-resistant strain harbors a constitutively expressed luminescent tag that enables the colonization pattern to be followed by bioluminescence imaging. Previous studies have shown strong correlation between cell numbers and bioluminescent signals (15, 43). Similarly, light levels emitted by bioluminescent *C. rodentium* strains have been shown to accurately reflect the bacterial numbers *in vivo* (55). *C. rodentium* strain ICC180 was cultured overnight in Luria-Bertani (LB) broth supplemented with NA (50µg/ml) (Sigma-Aldrich Ltd, Dublin, Ireland) @ 37°C, centrifuged @ 3000 *g* for 10 min and re-suspended in 10ml of sterile phosphate buffered saline (PBS) for oral gavage. Each mouse received 200µl (approximately 5 x 10^9 bacteria) of the bacterial suspension. Post-gavage, the remainder of the suspension was plated in serial

dilutions for retrospective enumeration. For bacterial enumeration in the stool collected at different time-points, serial dilutions of a fecal/PBS suspension (neat to 10^{-7}) were plated onto supplemented LB agar using a spot-plate technique and incubated overnight @ 37°C. To determine bacterial number in the spleen, the organ was weighed, manually crushed in 2ml of PBS in a stomacher bag, plated using serial dilutions onto supplemented LB agar and incubated overnight @ 37°C.

FTY720 administration

To assess the effect of continuous dosing of FTY720 on *C. rodentium*-induced colitis, mice were orally gavaged with vehicle (1% methylcellulose, Sigma-Aldrich Ltd, Dorset, England) or 3mg/kg FTY720 for 6 days pre-infection (day -6 to day -1 inclusive). Mice were orally gavaged with *C. rodentium* on day 0 and vehicle/ FTY720 dosing was continued every 2nd day from day 1 up until day 12 post-infection (p.i.). Mice were sacrificed at two time-points on day 8 (peak infection) and on day 14 (late infection/ clearance). The number of mice per group per time-point was 7. Non-infected controls were dosed with vehicle and FTY720 according to the same regime, n=4 per group. The FTY720 compound was kindly provided by Dr. A. Haynes (GlaxoSmithKline, Stevenage, UK).

In a separate study, we investigated the effect of stopping FTY720 dosing during early *C. rodentium* infection. In this instance, as with the continuous dosing study, the mice were orally gavaged daily with vehicle (1% methylcellulose) or 3mg/kg FTY720 for 6 days pre-infection (day -6 to day-1 inclusive). Following infection on day 0, dosing was continued for only 2 days. Mice were sacrificed on day 14. Number of mice per group was 7.

Clinical assessment of inflammation

Body weight was monitored regularly. Clinical assessment of inflammation was adapted from other colitis models (38, 39). Briefly, stool consistency (0=normal, well-formed pellets, 1=changed formed pellets, 2=loose stool, 3=diarrhea) and fur texture/posture (0=smooth coat/ not hunched, 1=mildly scruffy/mildly hunched, 2=very scruffy/very hunched) were recorded every 2nd day for the duration of the study to generate a disease activity index.

***In vivo* bioluminescence imaging**

On day 8 and 14 p.i., *in vivo* bioluminescence imaging was performed as previously described (10, 51), using an *IVIS* 100 charge-coupled device imaging system (Xenogen, Alameda, CA). Briefly, following gaseous anesthesia with 3% isoflurane, the animals were transferred to the imaging chamber where emission images were collected with 5 min integration times. Following the whole-body imaging, the mice were euthanized via cardiac puncture. The colons were removed, detached from the caecums, cut longitudinally, washed in PBS and imaged for 5 min. The caecums were also washed in PBS prior to imaging. The mesenteric lymph nodes (MLNs) and spleens were removed and imaged. Bioluminescent signal was quantified by creation of regions of interest (ROIs). To standardize the data, light emission was quantified from the same surface area (ROI) for each organ type. In addition, background light emission, taken from ROIs created on organs of non-infected control animals, was subtracted from test organs. Imaging data was analyzed and quantified with Living Image Software (Xenogen) and expressed as photons/second/cm^2.

Histology

The colons were removed, opened longitudinally, washed in PBS and separated into proximal and distal sections. The length of each colon was measured and 3cm was taken as the distal. The proximal and distal colons were weighed, cut longitudinally and one section of the distal was processed as a "Swiss roll" and snap frozen in OCT compound (Tissue-Tek, Sakura Finetek, USA) using liquid nitrogen. Frozen colons were cryo-sectioned (6μm), fixed for 5 min in ice-cold acetone/ethanol (3:1 ratio) and stained with haematoxylin and eosin according to standard histological procedures. Colon sections were evaluated and assigned scores in a blinded fashion for evidence of inflammatory damage such as goblet cell loss, crypt elongation, mucosal thickening and epithelial injury including hyperplasia and enterocyte shedding into the gut lumen. Scores were determined for four fields of view per mouse at 20x magnification (Olympus BX51, Germany) based on a scale of 0-3 (0=none, 1=mild, 2=moderate, 3=severe). A mean inflammatory score was then assigned per mouse distal colon, n= 3-4 mice per group.

Immunofluorescent staining

Frozen colon and MLN sections (6μm) were fixed in ice-cold acetone/alcohol mix (3:1 ratio), blocked with blocking serum for 45 min at room temperature in a humidified chamber and stained with combinations of the mAbs listed in Table 1. Purified mAbs were counter-stained using the appropriate AlexaFluor488-conjugated anti-Ig antibody (Invitrogen, BioSciences Ltd**,** Ireland). Hoechst (Invitrogen) was used as a nuclear counter-stain. Stained sections were mounted in ProLong Gold antifade reagent (Invitrogen) and were coded and visualized using a fluorescent

microscope (Olympus BX51, Germany) in a blinded fashion. For cell number quantitation, 7-10 fields of view were counted @ 40X for 3-4 mice per group.

Flow Cytometry

Blood was harvested from the mice via cardiac puncture on day 8 and day 14 into 0.01M EDTA (Sigma-Aldrich) and lysed in 2ml ACK (buffered ammonium chloride) lysis buffer (0.15M NH_4Cl / 1mM $KHCO_3$ / 0.1mM EDTA, pH 7.2). Following centrifugation, the red layer was removed leaving the clear pellet containing the white blood cells. A final concentration of 2 x 10^5 cells/well was re-suspended in blocking buffer. To this cell suspension; 50µL of each mAb dye mix was added with incubation in the dark at 4^{o}C for 30 min. Combinations of the mAbs listed in Table 1 were used in this study. Following staining, the cells were washed twice with blocking buffer and fixed in 1% paraformaldehyde. Relative fluorescence intensities were measured using a LSRII cytometer and BD Diva software (Becton Dickinson, UK). For each sample, 10-20,000 events were recorded. The percentage of cells labeled with each mAb was calculated in comparison with cells stained with isotype control antibody. Analysis gates for each antibody were set by using FMO (fluorescence minus one) controls with a threshold below 1%. The results represent the percentage of positively stained cells in the total cell population exceeding the background staining signal.

RNA extraction and quantitative RT-PCR (qRT-PCR)

Colonic mucosal mRNA expression was evaluated using qRT-PCR. The distal colons were weighed, cut longitudinally and one section was snap frozen in 1ml RNA later. Frozen colonic tissue samples were thawed on ice and transferred to magnalyser tubes with green beads (Roche Ireland Limited, Clare, Ireland) containing 1ml of lysis

buffer (provided by mirVana kit, Ambion, Applied Biosystems). Samples were homogenized (x3) @ 6,500 *g* for 15 seconds using a Magnalyser Instrument (Roche). Homogenized samples were centrifuged @ 200 *g* for 5 min @ 4°C and the supernatants were stored @ -80°C. Total RNA was isolated from colonic tissue homogenates using mirVana Kit, according to the manufacturers' protocol. RNA purity was measured by spectrophotometric analysis using a nanodrop. Complementary DNA (cDNA) was synthesized using 1µg total RNA. PCR primers and probes were designed using the Universal ProbeLibrary Assay Design Centre (https://www.roche-applied-science.com/sis/rtpcr/upl/adcs.jsp). Assays were designed for murine *Il-1β, Il-12p40, Il-6, Il-4, Il-10, Il-17a, Il-22, Il-23a, NOS2* (iNOS)*, Ifn-γ, Rorc* (retinoic acid-related orphan receptor gamma t, RORγt), *Tbx21* (Tbet)*, Tnf-α, Foxp3* and *RegIIIγ.* Primer sequences and corresponding probe numbers are available upon request. β-actin was used as housekeeping gene to correct for variability in the initial amount of total RNA. All PCR reactions were performed in triplicate using 384-well plates on the LightCycler 480 System (Roche). Positive and negative controls were also included. The $2^{-\Delta\Delta Ct}$ method (33) was used to calculate relative changes in gene expression determined from qRTPCR experiments.

Statistical Analysis

Data are represented by Mean ± SEM unless otherwise stated. The specific tests used are as indicated in the figure legends. All statistical tests were performed using commercially available statistic software (GraphPad Software Inc, CA). A *P* value of < 0.05 was considered significant.

RESULTS

FTY720 induces peripheral blood lymphopenia by trapping lymphocytes within the LNs

The effect of FTY720 on blood immune cell populations in *C. rodentium* infected mice was assessed at various time-points during the treatment period using flow cytometry. A significant reduction of T cells in the blood (lymphopenia) was observed in the FTY720-treated animals, compared to those that received vehicle on day 8 and day 14 p.i. (Fig. 1A), in accordance with previous reports (35). A similar reduction was observed with levels of B cells on day 8, but not on day 14 p.i. (Fig. 1A). Additionally, a significant increase in DCs was observed in the blood of the FTY720-treated mice on day 14 p.i., but not on day 8 p.i. (Fig. 1A). FTY720 treatment appeared to have no effect on levels of blood granulocytes (Fig. 1A), monocytes, NK or NKT cells (data not shown) on either of the time-points analyzed. Non-infected controls treated with the same dosing regime of vehicle or FTY720 showed similar results on day 14 (Supplemental Fig. 1A).

Immunofluorescent staining of frozen tissue sections demonstrated a marked accumulation of $CD3^+$ T cells in the MLNs of FTY720-treated mice on day 14 p.i., confirming the inhibitory effect of the S1P analogue on their egress from secondary lymphoid organs (Fig. 1B).

FTY720 treatment increases pathogen burden and impairs bacterial clearance

To determine the effects of FTY720 on *C. rodentium* infection in mice, we visualized and quantitated levels and tissue distribution of the pathogen on day 8 and day 14 p.i. using bioluminescence imaging. Whole-body imaging revealed a high pathogen burden in the lower abdominal/ gastrointestinal region of both the vehicle-treated and

FTY720-treated mice on day 8 p.i. (Fig. 2A). However, the bioluminescent signal from the FTY720-treated animals was significantly higher ($p<0.001$, Fig. 2A and C). On day 14 p.i., while whole-body imaging revealed clearance of the bacteria by the infected vehicle-treated mice, as evidenced by a significantly diminished bioluminescent signal, no such clearance was evident in the infected FTY720-treated mice (Fig. 2B and C). *Ex vivo* bioluminescence imaging of the organs on day 8 p.i. revealed significantly higher colonization of caecums ($p<0.05$), colons ($p<0.05$), spleens ($p<0.01$) and MLNs ($p<0.001$) of the FTY720-treated mice compared to the vehicle-treated (Fig. 2D). *C. rodentium* initially infects the caecum and then moves onto the distal colon. We and others have confirmed this colonisation pattern using bioluminescence (55). In the present study, 100% of the FTY720-treated mice had evidence of bacteria in the caecum on day 8 p.i., compared to 28% of those that received vehicle. By day 14 p.i., in contrast to the vehicle-treated mice, the signal from the colons and caecums remained high in the FTY720-treated animals and there was evidence of MLN infection in just under half of the mice (Fig. 2D). The bioluminescence data were supported by fecal cfu counts, which were performed at various time-points p.i.. These confirmed that day 8 was close to peak infection (Fig. 2E). In addition, FTY720-treated mice shed significantly higher numbers of *C. rodentium* in their stool from day 9 p.i. on, compared with vehicle-treated controls, and showed no signs of clearing the infection. Bacterial numbers in the feces of the drug-treated animals continued to increase over-time (Fig. 2E), while those of the vehicle-treated animals began to drop after day 7 p.i.. Splenic bacterial counts were similar between vehicle-treated and FTY720-treated animals on day 8 p.i.. However, on day 14 p.i. the vehicle-treated animals no longer had any evidence of bacterial growth in this organ, while bacterial burden in the spleen of mice receiving the S1P

analogue remained high (Fig. 2F). In contrast to vehicle-treated mice, FTY720-treated animals did not resolve the infection by day 14 p.i. and still had high concentrations of bacteria in all organs analyzed.

FTY720 treatment exacerbates clinical and colonic pathology during *C. rodentium* infection

To determine the effect of FTY720 administration on disease during *C. rodentium* infection, we monitored clinical and macroscopic signs of inflammation post-infection. In all mice infected with *C. rodentium*, weight loss was absent or minimal (Supplemental Fig. 2A) and the disease activity scores were well below the maximum possible, i.e. 5 on the scale used (mean 0.4 at day 8 p.i. and 0.9 on day 14 p.i. in vehicle treated mice, respectively, Supplemental Fig. 2B). Nevertheless, there was a significant increase in the disease activity score of infected FTY720-treated mice on days 7 ($p<0.01$), 8 ($p<0.01$) and 10 ($p<0.05$) p.i., respectively compared to infected vehicle-treated (Supplementary Fig. 2B). These time-points are considered to represent peak infection with the bacteria. No differences in colon length were evident between the vehicle-treated (5.8cm ± 0.2cm) and FTY720-treated groups (5.9cm ± 0.1cm) on day 14 p.i.. At necropsy, changes in distal colonic weight were assessed as an indirect measurement of epithelial hyperplasia, mucosal inflammation and hyperaemia, all of which are common features of *C. rodentium* infection. Animals infected with *C. rodentium* had significantly heavier distal colons, than their non-infected counterparts, on both time-points analyzed, i.e. day 8 ($p<0.05$) and day 14 p.i. ($p<0.001$) (Fig. 3A). Moreover, no differences in distal colonic weights were observed between vehicle-treated and FTY720-treated non-infected controls (Supplementary Figure 1B). In contrast, *C. rodentium*-infected mice that received

FTY720 had heavier distal colons, than those treated with vehicle on day 14 p.i., suggesting increased inflammation. This observation was supported by histological analysis of the distal colons, which revealed significantly increased inflammatory score, i.e. higher mucosal thickening, epithelial cell hyperplasia and goblet cell depletion, in the infected FTY720-treated mice compared to infected vehicle-treated controls (Fig. 3B and C). Although signs of inflammation and tissue damage were evident in the vehicle-treated colons compared to the non-infected colons at day 14 p.i., it was much less severe and resolution and epithelial healing appeared to be taking place.

FTY720 alters the composition of immune cell populations infiltrating the colon during *C. rodentium* infection

To determine the effect of FTY720 on the composition and distribution of immune cell populations in the colon during *C. rodentium* infection, frozen colonic sections were fluorescently stained and analysed for the number of $CD3^+$ T cells, $CD19^+$ B cells, $CD11c^+$ DCs, $F4/80^+$ macrophages and $Ly6G^+$ neutrophils. A marked increase in T cells ($p<0.001$), B cells ($p<0.05$), DCs ($p<0.001$), macrophages ($p<0.001$) and neutrophils ($p<0.01$) was observed within the distal colons of vehicle-treated animals compared to non-infected controls on day 14 p.i. (Fig. 4A and B). In comparison to the vehicle-treated animals, T and B lymphocytes ($p<0.01$, $p<0.001$), DCs ($p<0.01$) and macrophages ($p<0.001$) were significantly decreased in the distal colons of FTY720-treated animals at this time-point (Fig. 4A and B). However, the numbers of neutrophils were significantly increased ($p<0.05$) in these mice (Fig. 4A and B).

FTY720 treatment down-regulates genes associated with the mucosal immune response to ***C. rodentium***

To assess the effect of FTY720 treatment on the expression of innate and adaptive immune-modulatory genes during *C. rodentium* infection, distal colonic RNA was isolated and mRNA expression was evaluated using qRT-PCR. In the distal colons of *C. rodentium*-infected animals that received vehicle, expression levels of innate immune genes, such as the pro-inflammatory mediators IL-1β, iNOS and TNF-α, were significantly up-regulated compared to non-infected controls at day 8 p.i.. This up-regulation was significantly decreased in FTY720-treated animals compared to vehicle-treated (Fig. 5A). In contrast, on day 14 p.i. the expression of these mediators, together with IL-17a and IL-6, was significantly up-regulated in the drug-treated animals compared to vehicle-treated controls at this time point (Fig. 5A). Similarly, TNF-α was also increased in these mice at this time point (p=0.053).Genes associated with an adaptive T cell response such as IL-23, IL-22, IL-4 and IL-10 were significantly decreased in infected vehicle-treated mice compared to non-infected controls at day 8 p.i.. This down-regulation was not significantly affected by FTY720-treatment at this time point (Fig. 5B). In contrast, gene expression of the Th1 cytokine IL-12p40 was significantly up-regulated in infected vehicle-treated mice compared to non-infected controls at day 14 p.i. However, a significant up-regulation of the other T-cell associated cytokine genes was not detected in infected vehicle-treated mice compared to non-infected mice at this time point. Nevertheless, colonic expression of IL-12p40, IFN-γ, IL-22, IL-10, IL-4, the Treg transcription factor Foxp3 and the Th17 inducers RORγt and IL-23 were significantly decreased in infected FTY720-treated compared to infected vehicle-treated mice at day 14 p.i. (Fig. 5B). No significant changes were observed on the expression of Tbet or REGIIIγ in infected FTY720-

treated compared to vehicle-treated animals. qRT-PCR on colonic gene expression was also carried out on vehicle-treated and FTY720-treated non-infected controls, but no significant changes were observed (data not shown).

Termination of FTY720 treatment at early time-points p.i. had minimal effects on peripheral blood lymphopenia or pathogen clearance.

To determine what effect termination of FTY720 dosing has during early *C. rodentium* infection, mice were administered vehicle or the S1P analogue daily for 6 days prior to *C. rodentium* infection and 2 days after infection. On day 14 p.i., blood leukocyte populations, colonization and clinical and macroscopic markers of infection were determined. In the infected mice that had been treated with FTY720, peripheral blood lymphopenia was maintained, as were the enhanced numbers of DCs (Fig. 6A). Unlike with continuous dosing p.i., blood levels of peripheral granulocytes and NK cells were increased compared to the infected vehicle-treated mice (Fig. 6A). Whole-body bioluminescence imaging revealed that the FTY720-treated mice were still heavily colonized by day 14 p.i. and had higher signals from their colon ($p<0.001$, Fig. 6C and D), caecum ($p<0.001$, Fig. 6C and Supplemental Fig. 3), MLNs and spleen ($p<0.001$, Supplemental Fig. 3). These data were supported by faecal cfu counts (Fig. 6E). However, no differences in disease activity or distal colon weight were evident between the infected vehicle-treated group and those that had received FTY20.

Discussion

The results of this study show that FTY720 delayed clearance of the murine enteric pathogen *C. rodentium*. This was most likely a result of FTY720-mediated peripheral lymphopenia and T cell entrapment within the lymph nodes resulting in impairment of the adaptive immune response within the colon. Additionally, the colonic innate immune response was impaired and there was increased colon pathology and bacterial dissemination.

Our data show that FTY720 induced peripheral blood lymphopenia pre- and post-infection and T cell entrapment within the MLNs, which is consistent with previous reports (1, 3). Data from bioluminescence imaging of whole-body and organs combined with viable bacterial counts of the stool and spleen revealed that FTY720-treated mice were highly susceptible to colonic and systemic infection with *C. rodentium*. In addition to increased bacterial burden, more extensive pathogen distribution and impaired bacterial clearance, these mice exhibited higher disease activity at peak infection and greater colonic pathology at day 14 p.i.. These findings are in contrast to what has been previously demonstrated in experimental models of colitis reflecting IBD (11, 12, 14, 18, 36). In these instances, FTY720 had a therapeutic effect on disease by blunting immunity. In the present study, FTY720 blocked lymphocyte migration to the *C. rodentium*-infected intestine. Notably, FTY720-treated mice had reduced numbers of colonic T cells, DCs, B cells and macrophages, but increased numbers of neutrophils at day 14 p.i. when compared to vehicle-treated infected controls. These results are reminiscent of those observed in T and B cell deficient RAG1 knockout (KO) mice (45). In fact, *C. rodentium* infection

in these mice also leads to a predominantly granulocytic colonic infiltrate and enhanced bacterial presence in peripheral organs as well as colons (34, 45, 54).

Neutrophils are important in the early innate immune response to infection such as *C. rodentium*, preventing dissemination and controlling bacterial load (32, 50). However, during chronic inflammatory disease they can contribute to host tissue pathology (26, 41, 49). In the present study, increased neutrophil presence in the infected colons of FTY720-treated mice at day 14 p.i. was accompanied by enhanced severity of colonic inflammation. Interestingly, this increased neutrophil influx was also associated with up-regulated expression of the innate immune-related genes IL-1β, iNOS, IL-17a, IL-6 and TNF-α at day 14 p.i.. In agreement with previous reports, we found that gene expression of these innate immune cytokines was elevated in infected vehicle-treated mice compared to non-infected controls at peak infection (22, 48). These cytokines play a significant role in host defense and clearance of *C. rodentium* during early infection (13, 20, 25, 53). In the present study, it is possible that the innate immune response may be attempting to compensate for the blunted adaptive response in the infected FTY720-treated colons at day 14 p.i (32). Another possibility is that FTY720 is impairing the innate immune response at peak infection; a notion supported by the down-regulation of these cytokines in the FTY720-treated colons compared to vehicle-treated at day 8. The fact that the delayed innate response is unsuccessful at day 14 p.i. does not preclude the possibility that at later time-points, the heightened neutrophilic response may eventually promote clearance of *C. rodentium*. However, it should be noted that long-term infected RAG1KO mice (up to day 60 p.i.) also fail to clear *C. rodentium* infection(54).

The reduction in T cells, DCs and macrophages in the colons of the infected FTY720-treated mice at day 14 was in accordance with the decreased colonic mRNA expression of IL-12p40, IFN-γ, IL-23, IL-22, IL-4, IL-10, Foxp3 and RORγt in these mice at this time point. *C. rodentium* infection is associated with a highly polarized Th1 host immune response (22) and IL-12p40 is essential for adequate clearance of the pathogen from the gut (46). The cytokines IFN-γ (44), IL-22 and IL-23 (57) also play important roles in host defense against *C. rodentium* and their down-regulation in FTY720-treated animals may have contributed to the increased bacterial burden and dissemination. However, with the exception of IL-12p40, we did not see infection-specific induction of the other T cell-associated cytokines analyzed at day 8 or day 14 p.i.. This may be due to the kinetics of the immune response in the model and the time-points analyzed in this study.

Importantly, we also demonstrated that termination of FTY720 treatment early after infection had little or no effect on pathogen clearance or immune profiles. This data highlights that within a clinical setting; even with early diagnosis of infection, patients might still be highly susceptible to disease for at least two weeks or longer after termination of drug treatment.

To our knowledge, this is the first study investigating the effect of FTY720 treatment on a model of gastrointestinal infection. Previous studies using virus or antigen-specific virus inducers have suggested a risk of FTY720 in impairing immune responses (23, 42). Apart from the two fatalities reported, clinical studies in MS patients have found no other major complications regarding risk of infections, except for a higher incidence of lower respiratory tract and lung infection in patients treated

with FTY720 compared to placebo-treated (8, 28). However, based on the current study, vigilance should be maintained for bacterial infections, especially in patients with other autoimmune or intestinal inflammatory conditions where FTY720 may be considered a future therapeutic treatment. Further studies examining the effects of FTY720 treatment on antigen-specific immune responses upon exposure to a range of viral and bacterial infections are therefore required.

ACKNOWLEDGEMENTS

The Alimentary Pharmabiotic Centre is a research centre funded by Science Foundation Ireland (SFI). The authors and their work are supported by SFI grant numbers: 02/CE/B124 and 07/CE/B1368.

REFERENCES

1. **Brinkmann, V., A. Billich, T. Baumruker, P. Heining, R. Schmouder, G. Francis, S. Aradhye, and P. Burtin.** 2010. Fingolimod (FTY720): discovery and development of an oral drug to treat multiple sclerosis. Nat Rev Drug Discov **9:**883-897.
2. **Brinkmann, V., M. D. Davis, C. E. Heise, R. Albert, S. Cottens, R. Hof, C. Bruns, E. Prieschl, T. Baumruker, P. Hiestand, C. A. Foster, M. Zollinger, and K. R. Lynch.** 2002. The immune modulator FTY720 targets sphingosine 1-phosphate receptors. J Biol Chem **277:**21453-21457.
3. **Brinkmann, V., and K. R. Lynch.** 2002. FTY720: targeting G-protein-coupled receptors for sphingosine 1-phosphate in transplantation and autoimmunity. Curr Opin Immunol **14:**569-575.
4. **Budde, K., R. L. Schmouder, R. Brunkhorst, B. Nashan, P. W. Lucker, T. Mayer, S. Choudhury, A. Skerjanec, G. Kraus, and H. H. Neumayer.** 2002. First human trial of FTY720, a novel immunomodulator, in stable renal transplant patients. J Am Soc Nephrol **13:**1073-1083.
5. **Chi, H., and R. A. Flavell.** 2005. Cutting edge: regulation of T cell trafficking and primary immune responses by sphingosine 1-phosphate receptor 1. J Immunol **174:**2485-2488.
6. **Chiba, K., H. Matsuyuki, Y. Maeda, and K. Sugahara.** 2006. Role of sphingosine 1-phosphate receptor type 1 in lymphocyte egress from secondary lymphoid tissues and thymus. Cell Mol Immunol **3:**11-19.
7. **Cohen, J. A., F. Barkhof, G. Comi, H. P. Hartung, B. O. Khatri, X. Montalban, J. Pelletier, R. Capra, P. Gallo, G. Izquierdo, K. Tiel-Wilck, A. de Vera, J. Jin, T. Stites, S. Wu, S. Aradhye, and L. Kappos.** Oral fingolimod or intramuscular interferon for relapsing multiple sclerosis. N Engl J Med **362:**402-415.
8. **Collins, W., J. Cohen, P. O'Connor, A. de Vera, L. Zhang-Auberson, F. J. Jin, and L. Kappos.** 2010. Long-term safety of oral fingolimod (FTY720) in relapsing multiple sclerosis: integrated analyses of phase 2 and 3 studies. Mult Scler **16:**S295.
9. **Contag, C. H., P. R. Contag, J. I. Mullins, S. D. Spilman, D. K. Stevenson, and D. A. Benaron.** 1995. Photonic detection of bacterial pathogens in living hosts. Mol Microbiol **18:**593-603.
10. **Costa, G. L., M. R. Sandora, A. Nakajima, E. V. Nguyen, C. Taylor-Edwards, A. J. Slavin, C. H. Contag, C. G. Fathman, and J. M. Benson.** 2001. Adoptive immunotherapy of experimental autoimmune encephalomyelitis via T cell delivery of the IL-12 p40 subunit. J Immunol **167:**2379-2387.
11. **Daniel, C., N. Sartory, N. Zahn, G. Geisslinger, H. H. Radeke, and J. M. Stein.** 2007. FTY720 ameliorates Th1-mediated colitis in mice by directly affecting the functional activity of CD4+CD25+ regulatory T cells. J Immunol **178:**2458-2468.
12. **Daniel, C., N. A. Sartory, N. Zahn, R. Schmidt, G. Geisslinger, H. H. Radeke, and J. M. Stein.** 2007. FTY720 ameliorates oxazolone colitis in mice by directly affecting T helper type 2 functions. Mol Immunol **44:**3305-3316.
13. **Dann, S. M., M. E. Spehlmann, D. C. Hammond, M. Iimura, K. Hase, L. J. Choi, E. Hanson, and L. Eckmann.** 2008. IL-6-dependent mucosal

protection prevents establishment of a microbial niche for attaching/effacing lesion-forming enteric bacterial pathogens. J Immunol **180:**6816-6826.

14. **Deguchi, Y., A. Andoh, Y. Yagi, S. Bamba, O. Inatomi, T. Tsujikawa, and Y. Fujiyama.** 2006. The S1P receptor modulator FTY720 prevents the development of experimental colitis in mice. Oncol Rep **16:**699-703.
15. **Edinger, M., P. Hoffmann, C. H. Contag, and R. S. Negrin.** 2003. Evaluation of effector cell fate and function by in vivo bioluminescence imaging. Methods **31:**172-179.
16. **Eigenbrod, S., R. Derwand, V. Jakl, S. Endres, and A. Eigler.** 2006. Sphingosine kinase and sphingosine-1-phosphate regulate migration, endocytosis and apoptosis of dendritic cells. Immunol Invest **35:**149-165.
17. **Francis, K. P., J. Yu, C. Bellinger-Kawahara, D. Joh, M. J. Hawkinson, G. Xiao, T. F. Purchio, M. G. Caparon, M. Lipsitch, and P. R. Contag.** 2001. Visualizing pneumococcal infections in the lungs of live mice using bioluminescent Streptococcus pneumoniae transformed with a novel gram-positive lux transposon. Infect Immun **69:**3350-3358.
18. **Fujii, R., T. Kanai, Y. Nemoto, S. Makita, S. Oshima, R. Okamoto, K. Tsuchiya, T. Totsuka, and M. Watanabe.** 2006. FTY720 suppresses CD4+CD44highCD62L- effector memory T cell-mediated colitis. Am J Physiol Gastrointest Liver Physiol **291:**G267-274.
19. **Garber, K.** 2008. Infections cast cloud over Novartis' MS therapy. Nat Biotechnol **26:**844-845.
20. **Gobert, A. P., Y. Cheng, M. Akhtar, B. D. Mersey, D. R. Blumberg, R. K. Cross, R. Chaturvedi, C. B. Drachenberg, J. L. Boucher, A. Hacker, R. A. Casero, Jr., and K. T. Wilson.** 2004. Protective role of arginase in a mouse model of colitis. J Immunol **173:**2109-2117.
21. **Graler, M. H., and E. J. Goetzl.** 2004. The immunosuppressant FTY720 down-regulates sphingosine 1-phosphate G-protein-coupled receptors. Faseb J **18:**551-553.
22. **Higgins, L. M., G. Frankel, G. Douce, G. Dougan, and T. T. MacDonald.** 1999. Citrobacter rodentium infection in mice elicits a mucosal Th1 cytokine response and lesions similar to those in murine inflammatory bowel disease. Infect Immun **67:**3031-3039.
23. **Horga, A., J. Castillo, and X. Montalban.** 2010. Fingolimod for relapsing multiple sclerosis: an update. Expert Opin Pharmacother **11:**1183-1196.
24. **Hoshino, Y., C. Suzuki, M. Ohtsuki, Y. Masubuchi, Y. Amano, and K. Chiba.** 1996. FTY720, a novel immunosuppressant possessing unique mechanisms. II. Long-term graft survival induction in rat heterotopic cardiac allografts and synergistic effect in combination with cyclosporine A. Transplant Proc **28:**1060-1061.
25. **Ishigame, H., S. Kakuta, T. Nagai, M. Kadoki, A. Nambu, Y. Komiyama, N. Fujikado, Y. Tanahashi, A. Akitsu, H. Kotaki, K. Sudo, S. Nakae, C. Sasakawa, and Y. Iwakura.** 2009. Differential roles of interleukin-17A and -17F in host defense against mucoepithelial bacterial infection and allergic responses. Immunity **30:**108-119.
26. **Ito, R., M. Kita, M. Shin-Ya, T. Kishida, A. Urano, R. Takada, J. Sakagami, J. Imanishi, Y. Iwakura, T. Okanoue, T. Yoshikawa, K. Kataoka, and O. Mazda.** 2008. Involvement of IL-17A in the pathogenesis of DSS-induced colitis in mice. Biochem Biophys Res Commun **377:**12-16.

27. **Kappos, L., J. Antel, G. Comi, X. Montalban, P. O'Connor, C. H. Polman, T. Haas, A. A. Korn, G. Karlsson, and E. W. Radue.** 2006. Oral fingolimod (FTY720) for relapsing multiple sclerosis. N Engl J Med **355:**1124-1140.
28. **Kappos, L., E. W. Radue, P. O'Connor, C. Polman, R. Hohlfeld, P. Calabresi, K. Selmaj, C. Agoropoulou, M. Leyk, L. Zhang-Auberson, and P. Burtin.** 2010. A placebo-controlled trial of oral fingolimod in relapsing multiple sclerosis. N Engl J Med **362:**387-401.
29. **Kenny, B., R. DeVinney, M. Stein, D. J. Reinscheid, E. A. Frey, and B. B. Finlay.** 1997. Enteropathogenic E. coli (EPEC) transfers its receptor for intimate adherence into mammalian cells. Cell **91:**511-520.
30. **Kersh, E. N., W. Luo, D. R. Adams, J. Mitchell, J. G. Garcia-Lerma, S. Butera, T. Folks, and R. Otten.** 2009. Evaluation of the lymphocyte trafficking drug FTY720 in SHIVSF162P3-infected rhesus macaques. J Antimicrob Chemother **63:**758-762.
31. **Lan, Y. Y., A. De Creus, B. L. Colvin, M. Abe, V. Brinkmann, P. T. Coates, and A. W. Thomson.** 2005. The sphingosine-1-phosphate receptor agonist FTY720 modulates dendritic cell trafficking in vivo. Am J Transplant **5:**2649-2659.
32. **Lebeis, S. L., B. Bommarius, C. A. Parkos, M. A. Sherman, and D. Kalman.** 2007. TLR signaling mediated by MyD88 is required for a protective innate immune response by neutrophils to Citrobacter rodentium. J Immunol **179:**566-577.
33. **Livak, K. J., and T. D. Schmittgen.** 2001. Analysis of relative gene expression data using real-time quantitative PCR and the 2(-Delta Delta C(T)) Method. Methods **25:**402-408.
34. **Maaser, C., M. P. Housley, M. Iimura, J. R. Smith, B. A. Vallance, B. B. Finlay, J. R. Schreiber, N. M. Varki, M. F. Kagnoff, and L. Eckmann.** 2004. Clearance of Citrobacter rodentium requires B cells but not secretory immunoglobulin A (IgA) or IgM antibodies. Infect Immun **72:**3315-3324.
35. **Mehling, M., T. A. Johnson, J. Antel, L. Kappos, and A. Bar-Or.** 2011. Clinical immunology of the sphingosine 1-phosphate receptor modulator fingolimod (FTY720) in multiple sclerosis. Neurology **76:**S20-27.
36. **Mizushima, T., T. Ito, D. Kishi, Y. Kai, H. Tamagawa, R. Nezu, H. Kiyono, and H. Matsuda.** 2004. Therapeutic effects of a new lymphocyte homing reagent FTY720 in interleukin-10 gene-deficient mice with colitis. Inflamm Bowel Dis **10:**182-192.
37. **Mundy, R., T. T. MacDonald, G. Dougan, G. Frankel, and S. Wiles.** 2005. Citrobacter rodentium of mice and man. Cell Microbiol **7:**1697-1706.
38. **Murphy, C. T., G. Moloney, L. J. Hall, A. Quinlan, E. Faivre, P. Casey, F. Shanahan, S. Melgar, and K. Nally.** 2010. Use of bioluminescence imaging to track neutrophil migration and its inhibition in experimental colitis. Clin Exp Immunol **162:**188-196.
39. **Murphy, C. T., G. Moloney, J. Macsharry, A. Haynes, E. Faivre, A. Quinlan, P. G. McLean, K. Lee, L. O'Mahony, F. Shanahan, S. Melgar, and K. Nally.** 2010. Technical Advance: Function and efficacy of an {alpha}4-integrin antagonist using bioluminescence imaging to detect leukocyte trafficking in murine experimental colitis. J Leukoc Biol **88:**1271-1278.
40. **Rocchetta, H. L., C. J. Boylan, J. W. Foley, P. W. Iversen, D. L. LeTourneau, C. L. McMillian, P. R. Contag, D. E. Jenkins, and T. R.**

Parr, Jr. 2001. Validation of a noninvasive, real-time imaging technology using bioluminescent Escherichia coli in the neutropenic mouse thigh model of infection. Antimicrob Agents Chemother **45:**129-137.

41. **Sartor, R. B.** 1994. Cytokines in intestinal inflammation: pathophysiological and clinical considerations. Gastroenterology **106:**533-539.
42. **Schmouder, R., C. Boulton, N. Wang, and O. J. David.** 2010. Effects of fingolimod on antibody response following steady-state dosing in healthy volunteers: a 4-week randomised, placebo-controlled study (P412). Mult Scler **16 (suppl 10):**S135.
43. **Sheikh, A. Y., S. A. Lin, F. Cao, Y. Cao, K. E. van der Bogt, P. Chu, C. P. Chang, C. H. Contag, R. C. Robbins, and J. C. Wu.** 2007. Molecular imaging of bone marrow mononuclear cell homing and engraftment in ischemic myocardium. Stem Cells **25:**2677-2684.
44. **Shiomi, H., A. Masuda, S. Nishiumi, M. Nishida, T. Takagawa, Y. Shiomi, H. Kutsumi, R. S. Blumberg, T. Azuma, and M. Yoshida.** 2010. Gamma interferon produced by antigen-specific CD4+ T cells regulates the mucosal immune responses to Citrobacter rodentium infection. Infect Immun **78:**2653-2666.
45. **Simmons, C. P., S. Clare, M. Ghaem-Maghami, T. K. Uren, J. Rankin, A. Huett, R. Goldin, D. J. Lewis, T. T. MacDonald, R. A. Strugnell, G. Frankel, and G. Dougan.** 2003. Central role for B lymphocytes and CD4+ T cells in immunity to infection by the attaching and effacing pathogen Citrobacter rodentium. Infect Immun **71:**5077-5086.
46. **Simmons, C. P., N. S. Goncalves, M. Ghaem-Maghami, M. Bajaj-Elliott, S. Clare, B. Neves, G. Frankel, G. Dougan, and T. T. MacDonald.** 2002. Impaired resistance and enhanced pathology during infection with a noninvasive, attaching-effacing enteric bacterial pathogen, Citrobacter rodentium, in mice lacking IL-12 or IFN-gamma. J Immunol **168:**1804-1812.
47. **Sinha, R. K., C. Park, I. Y. Hwang, M. D. Davis, and J. H. Kehrl.** 2009. B lymphocytes exit lymph nodes through cortical lymphatic sinusoids by a mechanism independent of sphingosine-1-phosphate-mediated chemotaxis. Immunity **30:**434-446.
48. **Smith, A. D., S. Botero, T. Shea-Donohue, and J. F. Urban, Jr.** 2011. The pathogenicity of an enteric Citrobacter rodentium Infection is enhanced by deficiencies in the antioxidants selenium and vitamin E. Infect Immun **79:**1471-1478.
49. **Southey, A., S. Tanaka, T. Murakami, H. Miyoshi, T. Ishizuka, M. Sugiura, K. Kawashima, and T. Sugita.** 1997. Pathophysiological role of nitric oxide in rat experimental colitis. Int J Immunopharmacol **19:**669-676.
50. **Spehlmann, M. E., S. M. Dann, P. Hruz, E. Hanson, D. F. McCole, and L. Eckmann.** 2009. CXCR2-dependent mucosal neutrophil influx protects against colitis-associated diarrhea caused by an attaching/effacing lesion-forming bacterial pathogen. J Immunol **183:**3332-3343.
51. **Sweeney, T. J., V. Mailander, A. A. Tucker, A. B. Olomu, W. Zhang, Y. Cao, R. S. Negrin, and C. H. Contag.** 1999. Visualizing the kinetics of tumor-cell clearance in living animals. Proc Natl Acad Sci U S A **96:**12044-12049.
52. **Thangada, S., K. M. Khanna, V. A. Blaho, M. L. Oo, D. S. Im, C. Guo, L. Lefrancois, and T. Hla.** 2010. Cell-surface residence of sphingosine 1-

phosphate receptor 1 on lymphocytes determines lymphocyte egress kinetics. J Exp Med **207:**1475-1483.

53. **Vallance, B. A., W. Deng, M. De Grado, C. Chan, K. Jacobson, and B. B. Finlay.** 2002. Modulation of inducible nitric oxide synthase expression by the attaching and effacing bacterial pathogen citrobacter rodentium in infected mice. Infect Immun **70:**6424-6435.
54. **Vallance, B. A., W. Deng, L. A. Knodler, and B. B. Finlay.** 2002. Mice lacking T and B lymphocytes develop transient colitis and crypt hyperplasia yet suffer impaired bacterial clearance during Citrobacter rodentium infection. Infect Immun **70:**2070-2081.
55. **Wiles, S., S. Clare, J. Harker, A. Huett, D. Young, G. Dougan, and G. Frankel.** 2004. Organ specificity, colonization and clearance dynamics in vivo following oral challenges with the murine pathogen Citrobacter rodentium. Cell Microbiol **6:**963-972.
56. **Wolf, A. M., K. Eller, R. Zeiser, C. Durr, U. V. Gerlach, M. Sixt, L. Markut, G. Gastl, A. R. Rosenkranz, and D. Wolf.** 2009. The sphingosine 1-phosphate receptor agonist FTY720 potently inhibits regulatory T cell proliferation in vitro and in vivo. J Immunol **183:**3751-3760.
57. **Zheng, Y., P. A. Valdez, D. M. Danilenko, Y. Hu, S. M. Sa, Q. Gong, A. R. Abbas, Z. Modrusan, N. Ghilardi, F. J. de Sauvage, and W. Ouyang.** 2008. Interleukin-22 mediates early host defense against attaching and effacing bacterial pathogens. Nat Med **14:**282-289.
58. **Zhi, L., P. Kim, B. D. Thompson, C. Pitsillides, A. J. Bankovich, S. H. Yun, C. P. Lin, J. G. Cyster, and M. X. Wu.** 2011. FTY720 blocks egress of T cells in part by abrogation of their adhesion on the lymph node sinus. J Immunol **187:**2244-2251.

Footnotes: S.M and K.N. share joint senior authorship of this work.

Present address of L.J.H.: Institute of Food Research, Norwich Research Park, Colney, Norwich NR4 7UA, UK

List of Abbreviations:

DCs, dendritic cells; *E. coli, Escherichia coli;* EPEC enteropathogenic *E. coli*; EHEC, enterohaemorrhagic *E. coli*; KO, knock out; MLNs, mesenteric lymph nodes; MS, multiple sclerosis; p.i., post infection; RORγt, retinoic acid-related orphan receptor gamma t; ROIs, regions of interest; S1P, sphingosine-1-phosphate; Treg, regulatory T cells;

FIGURE LEGENDS

Figure 1. FTY720 induces peripheral blood lymphopenia by trapping T cells in MLNs. (A) Leukocytes were isolated from the blood of non-infected and C. rodentium-infected animals on day 8 (peak infection) and day 14 (clearance) p.i. and stained with flurochrome-labelled mAb. They were analysed by flow cytometry in which 10,000-20,000 events were recorded. Data represents the mean percentage of CD3+ (T cells), B220+ (B cells), CD11c+ (DCs), and Ly6G+ (neutrophils). Significance determined by one-way ANOVA followed by Bonferroni's multiple comparison test compared to vehicle controls ***P < 0.001; **P < 0.01; *P < 0.05; n= 4–7 individual mice. (B) FTY720 traps T cells and DCs within the MLNs. In situ visualization of leukocytes within the MLNs of non-infected and *C. rodentium*-infected vehicle-treated and FTY720-treated animals on day 14 p.i.. Tissue sections from 4 individual mice per group were analyzed by fluorescent microscopy. Frozen MLN sections (6μm) were fixed in acetone/ethanol and stained for CD11c (green), and co-stained with CD3 (red) and nuclei (blue). A representative picture for each group is shown. (Original magnification, x20). Scale bar is 200μm.

Figure 2: FTY720 treatment impairs clearance of *C. rodentium* infection. Whole-body bioluminescence imaging of vehicle-treated and FTY720-treated mice on (A) day 8 and (B) day 14 p.i. with *C. rodentium*. (C) Bioluminescent signal from the gastrointestinal region (*in vivo* whole-body imaging) and from (D) *ex vivo* organs; colon, caecum, MLN and spleen. Data is expressed as mean ± SEM for 7 individual animals per group. Significance determined by Mann Whitney U T test; ***P < 0.001; **P < 0.01; *P < 0.05. Colonization and clearance of *C. rodentium* in vehicle-treated and FTY720-treated mice as indicated by viable bacterial counts (colony

forming units/cfus) from (E) stool and (F) spleen. Samples were taken at different time-points for 14 days p.i. Data is expressed as the mean of 7–14 individual mice ± SEM. Significance was determined by the Kruskal-Wallis test followed by Dunn's multiple comparison test; **P < 0.01; *P < 0.05.

Figure 3. FTY720 treatment exacerbates colonic pathology during *C. rodentium* infection. (A) Differences in distal colon weight at day 8 and day 14 p.i. Data represents the mean of 4–7 individual mice ± SEM. Significance between groups was determined by one-way ANOVA followed by Bonferroni's multiple comparison test; # P<0.05 non-infected versus vehicle day 8, # # # P<0.001 non-infected versus vehicle day 14, * P<0.05 vehicle versus FTY720. (B) Representative histology tissue sections of distal colons on day 14 p.i. showing epithelial shedding (**1**), crypt elongation and goblet cell depletion (**2**) and mucosal thickening (**3**). Images are representative of 3-4 individual animals per group. Original magnification x40. Scale bar is 100μm. (C) Mean inflammatory scores of vehicle- or FTY720-treated mice on day 14 p.i. as determined by histological analysis of distal colonic sections. $^{\#}$P<0.05 non-infected versus vehicle infected, **P<0.01 vehicle versus FTY720 infected, n=3-4 mice per group.

Figure 4. FTY720 alters the composition of immune cell populations in the colon during infection. Tissue sections from 4 individual mice were analyzed on day 14 p.i. by fluorescent microscopy. (A) Serial frozen sections (6μm) were fixed in acetone/ethanol and stained for CD11c, F4/80 and CD19 (green), and co-stained with CD3, LY6G (red) and nuclei (blue). A representative picture for each group is shown. Original magnification, x40. Scale bar is 100μm. E indicates epithelium and S shows

submucosa. (B) Quantitation of cells/mm^2 of tissue. Bars represent means ± SEM of the total number of positive cells per mm^2. Values are based on 3-4 individual mice, measuring 7–10 fields at 40x magnification of distal colons. Significance between groups was determined by one-way ANOVA followed by Bonferroni's multiple comparison test; $^{\#}P < 0.05$; $^{\#\#}P<0.01$; $^{\#\#\#}P<0.001$ non-infected versus vehicle infected. *P<0.05; **P<0.01; and ***P<0.001 vehicle infected versus FTY720 infected.

Figure 5. FTY720 impairs the mucosal immune response to *C. rodentium* infection. Distal colon mRNA extracts were analyzed for innate immune gene expression (A) and adaptive immune gene expression (B) on day 8 and day 14 p.i.. The 2-ΔΔCT method was used to calculate relative changes in gene expression compared with the non-infected (control) group. Expression was determined as fold induction compared with β-actin housekeeper. Bars represent mean of 4-6 individual mice ± SEM. Significance determined by Mann-Whitney U T test. $^{\#\#}P < 0.01$; $^{\#}P < 0.05$ non-infected control versus vehicle infected, ***P < 0.001; **P < 0.01; *P < 0.05 vehicle infected versus FTY720 infected.

Figure 6. Termination of FTY720 treatment post-infection had minimal effects on peripheral blood lymphopenia or pathogen colonisation. (A) Percentage of leukocyte populations in the blood. Mice were treated with FTY720 or vehicle for 6 days prior to *C. rodentium* infection and 2 days p.i.. Leukocytes were isolated from the blood of vehicle-treated and FTY720-treated *C. rodentium*-infected animals on day 14 p.i. and stained with fluorochrome-labelled mAb. They were analyzed by flow cytometry in which 10,000-20,000 events were recorded. Data represents the mean

percentage of CD3 (T cells), CD11c (DCs), B220 (B cells), and Ly6G (neutrophils) positive cells at two time-points during *C. rodentium*-infection. Significance was determined using the Mann Whitney U T test to compare vehicle-treated (control) animals with FTY720-treated animals, ***P < 0.001; **P < 0.01;*P < 0.05; n=6-8 individual mice. Effect of FTY720 on pathogen burden and clearance of *C. rodentium* infection. Representative bioluminescence images of (B) whole-body and (C) *ex vivo* colons (co) and caecums (cae) of vehicle-treated and FTY720-treated mice day 14 p.i.. (D) Bioluminescent signal from colon. Data is expressed as mean ± SEM for 6-8 individual mice per group. Significance determined by Mann Whitney U T test; ***P < 0.001; **P < 0.01; P < 0.05. (E) Colonization and clearance of *C. rodentium* in vehicle-treated and FTY720-treated mice as indicated by viable bacterial counts (colony forming units/cfus) from stool. Samples were taken at different time-points for 14 days p.i.. Data is expressed as the mean of 6-8 individual mice ± SEM. Significance was determined by the Kruskal-Wallis test followed by Dunn's multiple comparison test; **P < 0.01; *P < 0.05.

Fig. 1

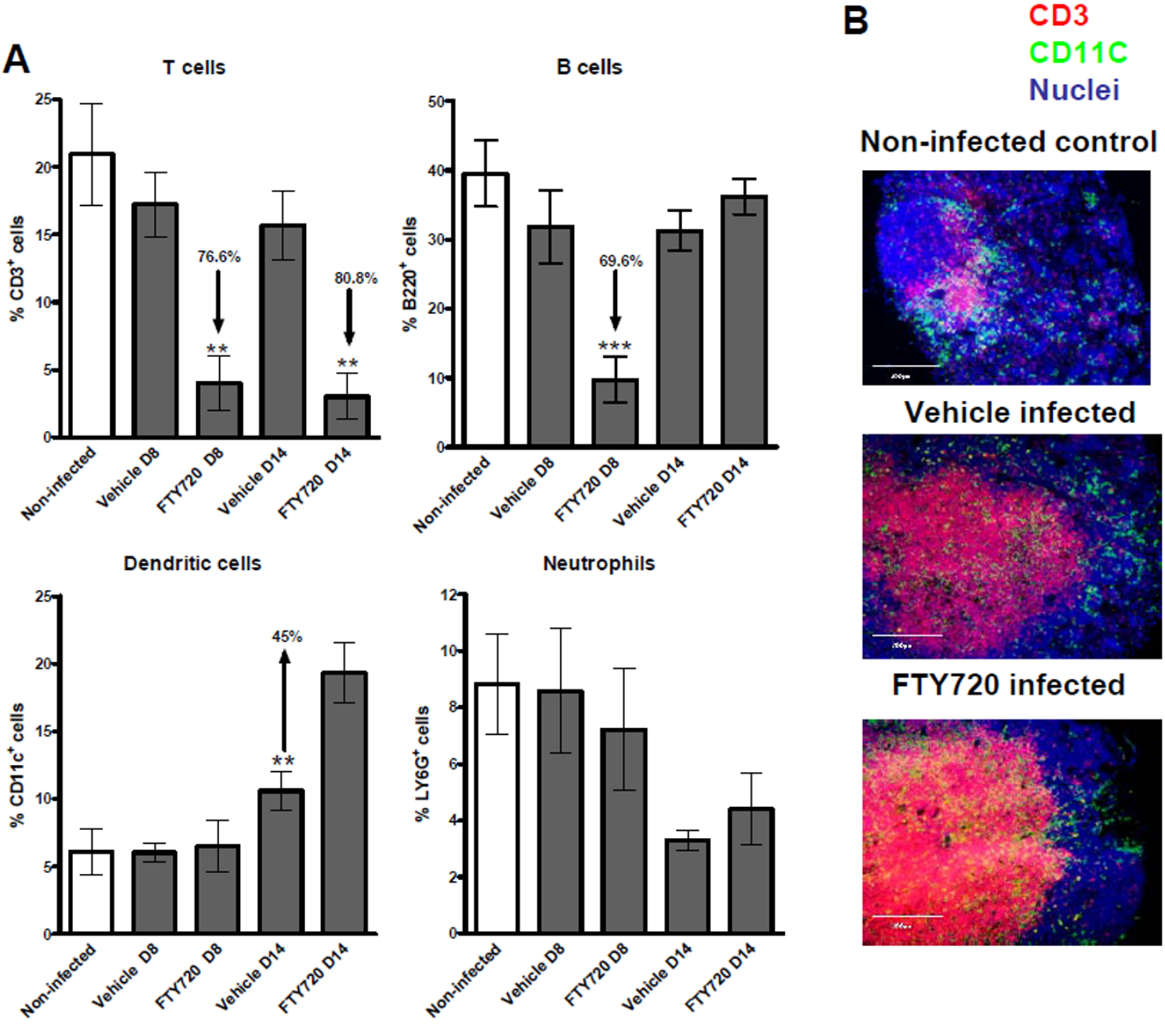
A
T cells
% CD3+ cells
76.6%
80.8%
**
**
Non-infected
Vehicle D8
FTY720 D8
Vehicle D14
FTY720 D14
B cells
% B220+ cells
69.6%
***
Dendritic cells
% CD11c+ cells
45%
**
Neutrophils
% LY6G+ cells
B
CD3
CD11C
Nuclei
Non-infected control
Vehicle infected
FTY720 infected

Fig. 2

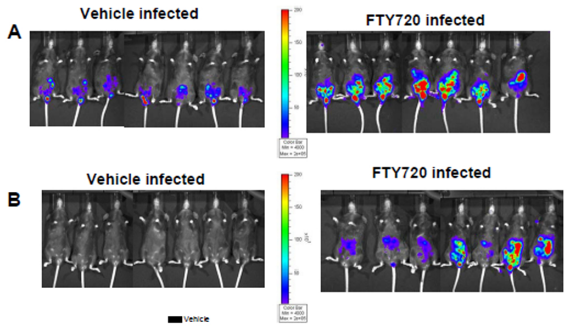
A
Vehicle infected
FTY720 infected
B
Vehicle infected
FTY720 infected

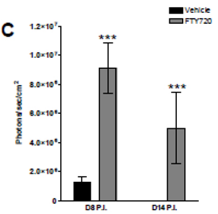
C
Vehicle
FTY720
Photons/sec/cm²
D8 P.I.
D14 P.I.

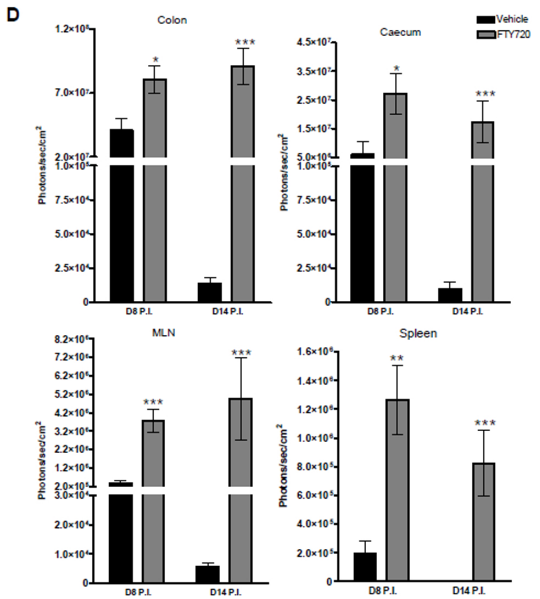
D
Colon
Caecum
MLN
Spleen
Vehicle
FTY720
Photons/sec/cm²
D8 P.I.
D14 P.I.

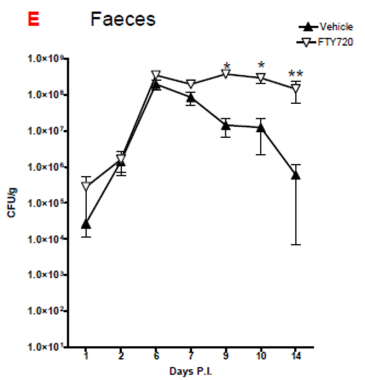
E
Faeces
Vehicle
FTY720
CFU/g
Days P.I.

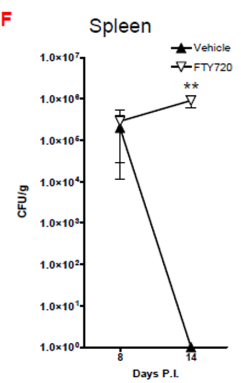
F
Spleen
Vehicle
FTY720
CFU/g
Days P.I.

Fig. 3

A

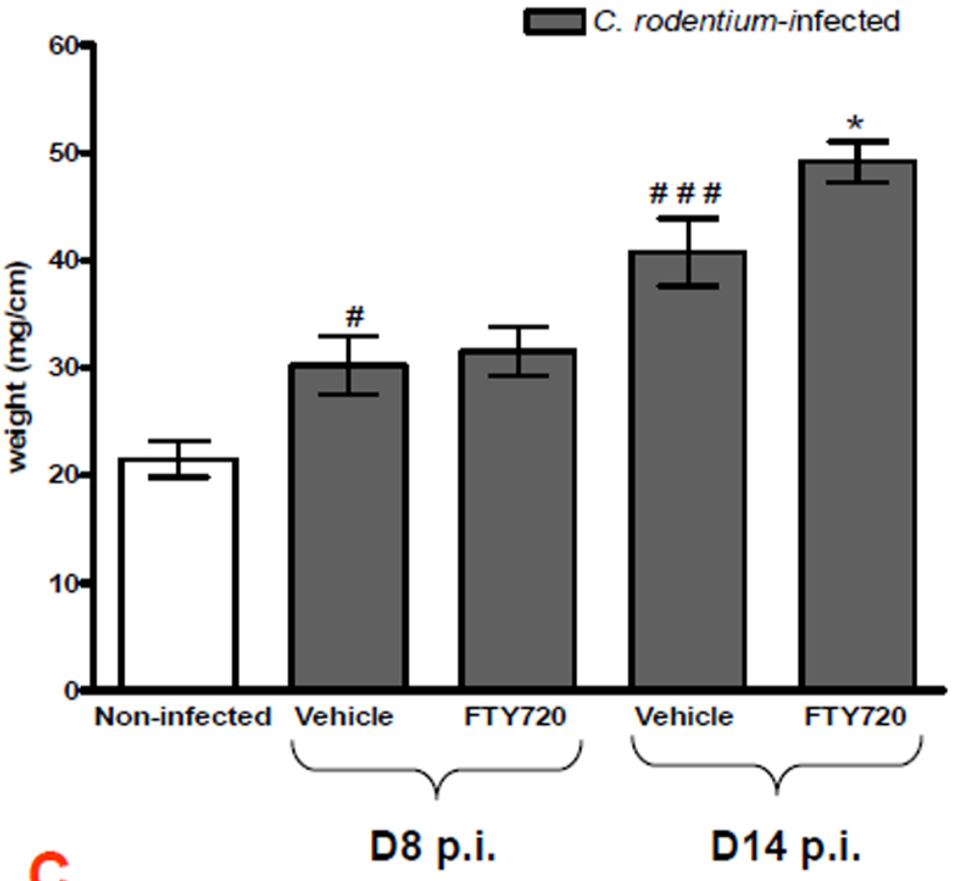
C. rodentium-infected
weight (mg/cm)
60
50
40
30
20
10
0
#
###
*
Non-infected
Vehicle
FTY720
Vehicle
FTY720
D8 p.i.
D14 p.i.

B


Non-infected
Vehicle infected
FTY720 infected
1
2
3

C

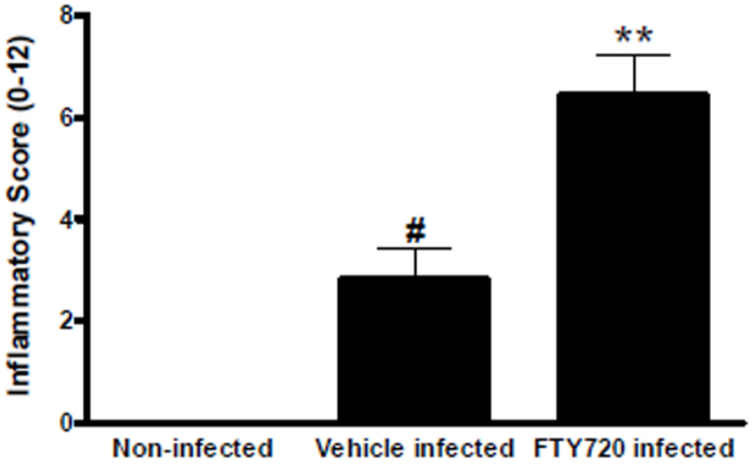
Inflammatory Score (0-12)
8
6
4
2
0
#
**
Non-infected
Vehicle infected
FTY720 infected

Fig. 4

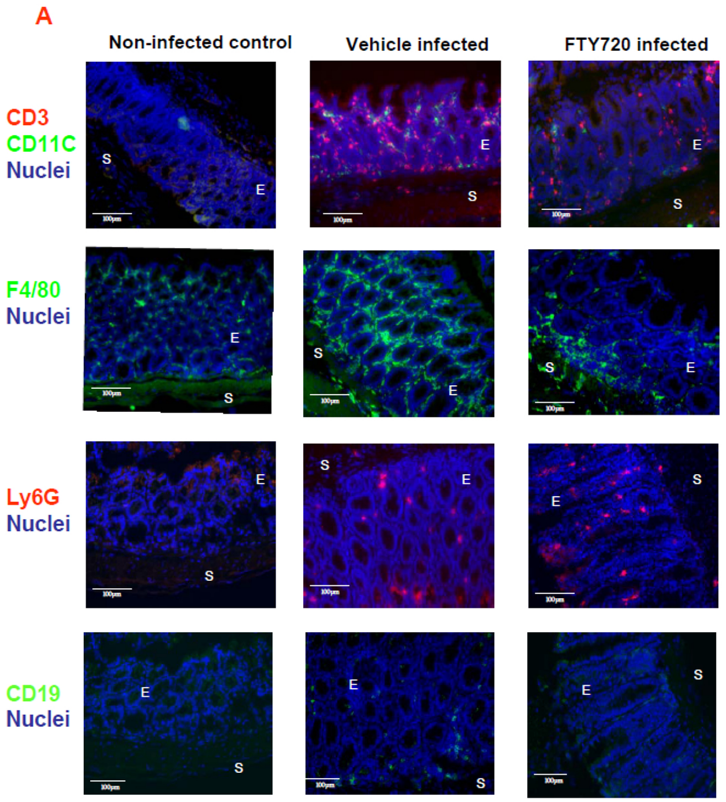
A
Non-infected control
Vehicle infected
FTY720 infected
CD3
CD11C
Nuclei
F4/80
Nuclei
Ly6G
Nuclei
CD19
Nuclei
E
S

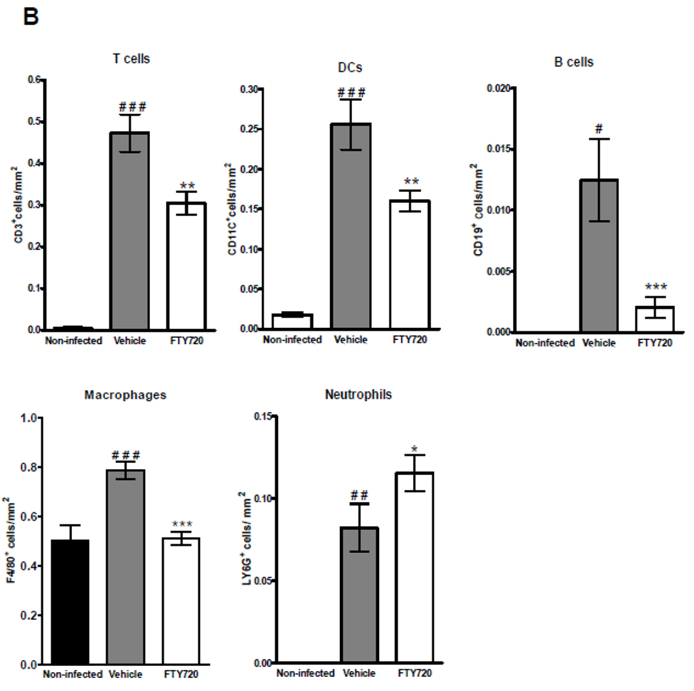
B
T cells
DCs
B cells
Macrophages
Neutrophils
Non-infected
Vehicle
FTY720
CD3+cells/mm2
CD11C+cells/mm2
CD19+ cells/mm2
F4/80+ cells/mm2
LY6G+ cells/ mm2

Figure 5

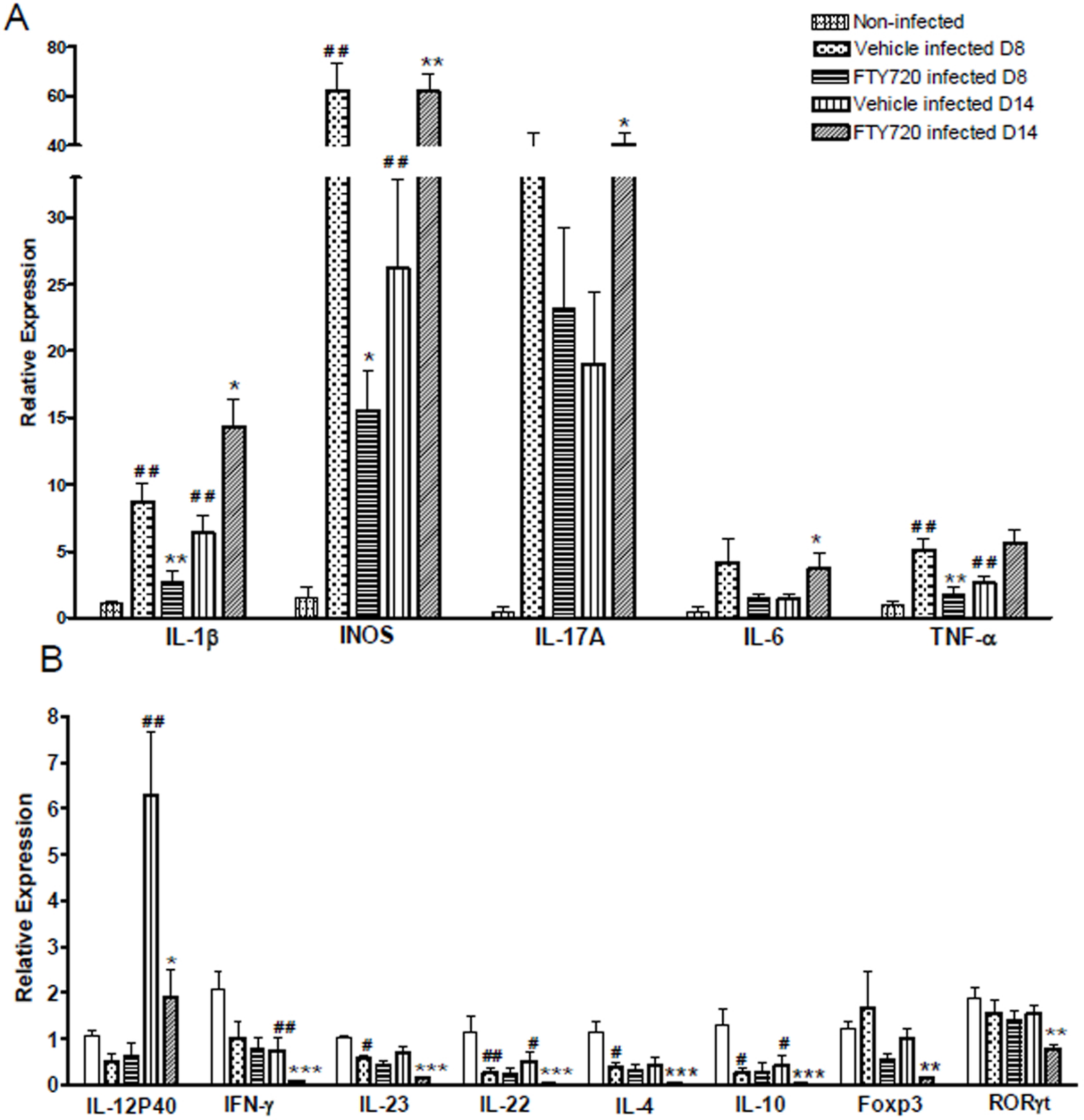
A
Non-infected
Vehicle infected D8
FTY720 infected D8
Vehicle infected D14
FTY720 infected D14
Relative Expression
IL-1β
INOS
IL-17A
IL-6
TNF-α
B
Relative Expression
IL-12P40
IFN-γ
IL-23
IL-22
IL-4
IL-10
Foxp3
RORγt

Fig. 6

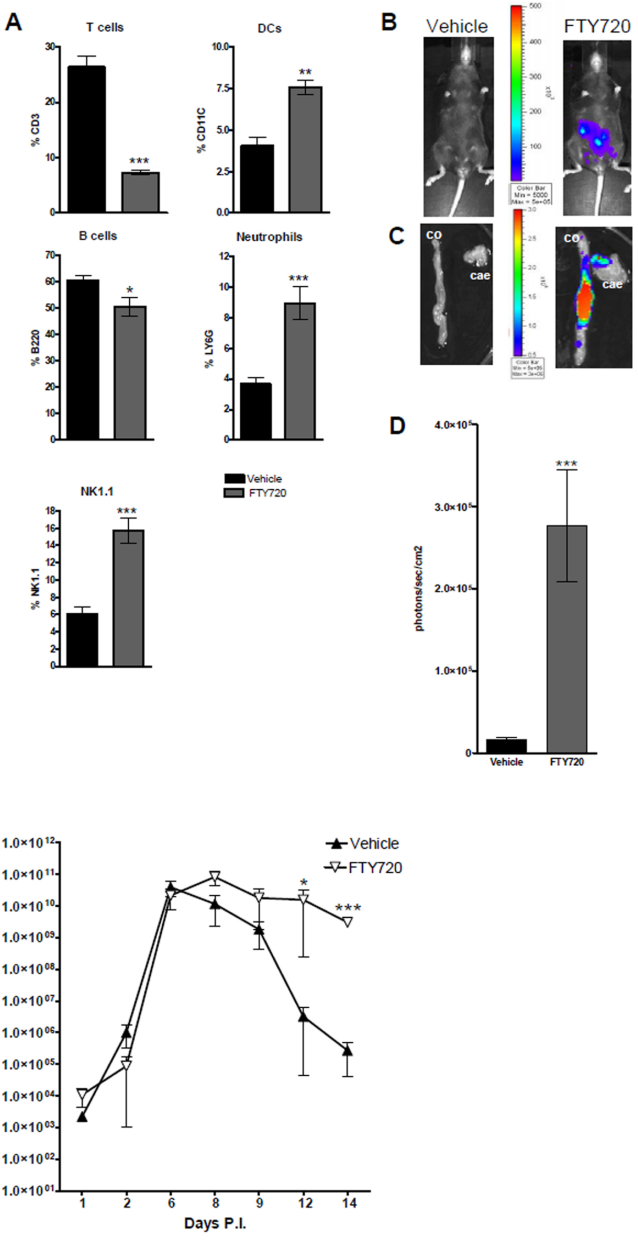
A
T cells
% CD3
***
DCs
% CD11C
**
B cells
% B220
*
Neutrophils
% LY6G
***
NK1.1
% NK1.1
***
Vehicle
FTY720
B
Vehicle
FTY720
C
co
cae
co
cae
D
photons/sec/cm2
***
Vehicle
FTY720
E
CFU/g
Vehicle
FTY720
*
***
Days P.I.

Table I. Antibodies used in this study

Target molecule	Host	Clone	Isotype	Conjugate	Source
CD3	Hamster	145-2C11	IgG1	APC	BD Biosciences
CD3	Hamster	145-2C11	IgG	PE	Biolegend
CD11c	Hamster	HL3	IgG1	PE	BD Biosciences
Ly6G	Rat	1A8	IgG2a	PE	BioLegend
CD19	Rat	6D5	IgG2a	None	BioLegend
B220	Rat	RA3-6B2	IgG2a	Alexafluor700	AbDSerotec
F4/80	Rat	CI:A3-1	IgG2b	None	Abcam
F4/80	Rat	BM8	IgG2b	TRI-COLOR	Caltag
NK1.1	Mouse	PK136	IgG2a	PerCp-CY5.5l	Biolegend
Rat IgG	Goat		IgG	Alexafluor488	Invitrogen
Rabbit IgG	Goat		IgG	Alexafluor488	Invitrogen